Soluble kagome Ising model in a magnetic field

W. T. Lu[1,2] and F. Y. Wu[1]
[1]*Department of Physics, Northeastern University, Boston, Massachusetts 02115, USA*
[2]*Electronic Materials Research Institute, Northeastern University, Boston, Massachusetts 02115, USA*
(Received 1 October 2004; published 18 April 2005)

An Ising model on the kagome lattice with superexchange interactions is solved exactly under the presence of a nonzero external magnetic field. The model generalizes the superexchange model introduced by Fisher in 1960 and is analyzed in light of a free-fermion model. We deduce the critical condition and present detailed analyses of its thermodynamic and magnetic properties. The system is found to exhibit a second-order transition with logarithmic singularities at criticality.

DOI: 10.1103/PhysRevE.71.046120 PACS number(s): 05.50.+q, 75.10.Hk, 04.20.Jb, 51.60.+a

I. INTRODUCTION

The Ising model in a nonzero magnetic field is a well-known unsolved problem in statistical mechanics. In 1960, Fisher [1] produced a remarkable solution of a superexchange antiferromagnetic Ising model in the presence of a nonzero field. The Fisher model is defined on a decorated square lattice where there is an external magnetic field applied to decorating spins which interact via superexchange interactions.

In this paper we consider similar superexchange models on the kagome lattice. The kagome lattice has been of interest in recent years in the role it plays in the high-T_c superconductivity. It has been known that special cases of the kagome Ising model are soluble in the presence of a magnetic field [2,3]. The structure of the ferrimagnet $SrCr_8Ga_4O_{19}$, for example, is found to consist of two-dimensional, spinel (kagome) slabs [4] with magnetic spins residing at $1/3$ of the lattice sites. Thus it is of interest to consider models with similar structures. Azaria and Giacomini [5] have extended the Fisher model by considering the kagome lattice shown in Fig. 1(a), which reduces to the Fisher model upon setting $K_1=0$. They obtained its partition function from which the phase diagram is deduced. But there has been no detailed discussion of its thermodynamic properties. Here, we consider yet another extension of the Fisher model to a kagome lattice as shown in Fig. 1(b). We show that the partition function of this model is identical to the Azaria and Giacomini solution [5]. We present detailed analyses of the thermodynamics of the solution which was not done in [5].

Consider an Ising model shown in Fig. 1(b) with an interaction energy

$$-J_1\sigma_1\sigma_2 + J(\sigma_2\sigma_3 - \sigma_3\sigma_1)$$

around every triangle formed by spins $\sigma_1,\sigma_2,\sigma_3$. Introduce reduced interactions $K=\beta J$, $K_1=\beta J_1$, where $\beta=1/kT$, such that $K,K_1>0$ indicate ferromagnetic interactions. In addition, there is an external magnetic field H applied to $2/3$ of the lattice sites denoted by solid circles. We denote the reduced field by $L=H/kT$. As a result, the magnetic spins interact with a superexchange interaction via intermediate nonmagnetic spins. It is clear that there is no loss of generality to restrict considerations to

$$H,J \geqslant 0 \text{ or } L,K \geqslant 0.$$

For $K_1=0$ the model reduces to the Fisher model for the square lattice. For $K_1\neq 0$ the present model is more general and differs from the Fisher model in a fundamental way as described in Sec. II below.

Our main result is a closed-form solution of the partition function and detailed analyses of thermodynamic and magnetic properties. In Sec. II we deduce the solution using a combination of star-triangle and decimation transformations. The phase diagram is analyzed in Sec. III. In Secs. IV–VI the internal energy, specific heat, magnetization, and susceptibility are analyzed using a free-fermion model formulation [6].

II. THE PARTITION FUNCTION

Denote the partition function of the kagome Ising lattice in Fig. 1(b) by $Z_{\mathrm{KG}}(K,K_1,L)$. Our main result is an equivalence of $Z_{\mathrm{KG}}(K,K_1,L)$ to the partition function of a honeycomb Ising model in zero field, a result which renders the model soluble.

This equivalence is established by effecting a sequence of spin transformations. First, we carry out a star-triangle transformation for every triangular face as shown in the first line in Fig. 2. This converts the kagome lattice to a decorated honeycomb lattice. Next the decorating spins are decimated as shown in the second and third lines in Fig. 2, and the lattice is reduced to that of a honeycomb. The crux of matter is that the external fields L_1 and $-L_1$ induced in the second step cancel out at the end. As a result, the final honeycomb lattice has *no* external field and is soluble. It has reduced interactions R,R, and R_1 in the three principal directions.

The transformations shown in Fig. 2 are standard [7,8]. For the transformation in the first line in Fig. 2, we have

$$e^{-2K-K_1} = 2F_1\cosh(\Gamma_1 + 2\Gamma), \tag{1}$$

$$e^{2K-K_1} = 2F_1\cosh(\Gamma_1 - 2\Gamma), \tag{2}$$

 ©2005 The American Physical Society

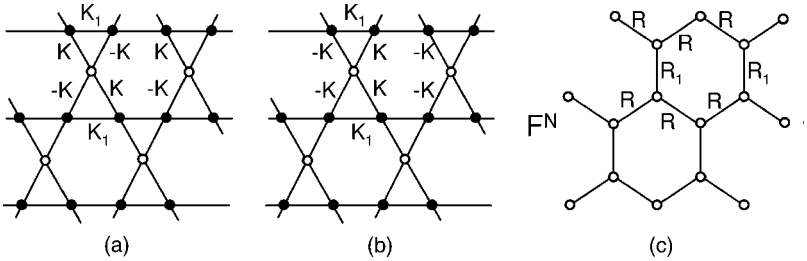

FIG. 1. (a) and (b) are two soluble kagome lattice Ising models in a magnetic field. Solid circles denote magnetic spins and open circles nonmagnetic spins. Both models are mapped to a honeycomb Ising lattice without a field shown in (c). F^N is an overall factor.

$$e^{K_1} = 2F_1 \cosh \Gamma_1, \tag{3}$$

from which we can solve Γ and Γ_1 in terms of K and K_1. Divide the sum and difference of Eqs. (1) and (2) by Eq. (3), we obtain, respectively,

$$\cosh 2\Gamma = e^{-2K_1} \cosh 2K, \tag{4}$$

$$\tanh \Gamma_1 = -\frac{e^{-2K_1} \sinh 2K}{\sinh 2\Gamma}. \tag{5}$$

We also obtain

$$F_1^4 = [16 \cosh^2 \Gamma_1 \cosh(\Gamma_1 + 2\Gamma) \cosh(\Gamma_1 - 2\Gamma)]^{-1}. \tag{6}$$

Now $K > 0$ and K_1 is real, so Eqs. (4) and (5) show that there are two regimes

$$e^{-2K_1} \cosh 2K > 1, \quad \text{regime I},$$

$$e^{-2K_1} \cosh 2K < 1, \quad \text{regime II}, \tag{7}$$

and Γ and Γ_1 are real in regime I and purely imaginary in regime II.

For the transformation in the second line in Fig. 2, we have

$$2 \cosh 2\Gamma_1 = F_2 e^{R_1},$$

$$2 = F_2 e^{-R_1}, \tag{8}$$

from which we obtain

$$F_2^2 = 4 \cosh 2\Gamma_1, \tag{9}$$

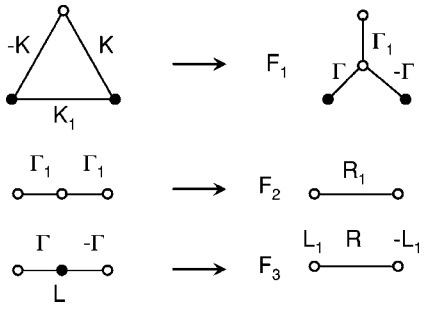

FIG. 2. Transformations used in deducing the mapping shown in Fig. 1. F_i, $i=1, 2, 3$, are constants.

$$e^{2R_1} = \cosh 2\Gamma_1 = \frac{e^{-4K_1} \cosh 4K - 1}{e^{-4K_1} - 1}, \tag{10}$$

where the last step is obtained after making use of Eq. (4). Equation (10) shows that R_1 is real, and $R_1 > 0$ in regime I and $R_1 < 0$ in regime II.

For the transformation in the third line in Fig. 2, we have

$$2 \cosh(L + 2\Gamma) = F_3 e^{-R+2L_1}, \tag{11}$$

$$2 \cosh(L - 2\Gamma) = F_3 e^{-R-2L_1}, \tag{12}$$

$$2 \cosh L = F_3 e^{R}, \tag{13}$$

from which we obtain

$$e^{-4R} = \frac{\cosh(L + 2\Gamma)\cosh(L - 2\Gamma)}{\cosh^2 L} = 1 + \frac{\sinh^2 2\Gamma}{\cosh^2 L}$$

$$= \frac{e^{-4K_1} \cosh^2 2K + \sinh^2 L}{\cosh^2 L}, \tag{14}$$

$$e^{4L_1} = \frac{\cosh(L + 2\Gamma)}{\cosh(L - 2\Gamma)}, \tag{15}$$

$$F_3^4 = 16 \cosh^2 L \cosh(L + 2\Gamma)\cosh(L - 2\Gamma). \tag{16}$$

Thus, R is always real, and we have

$$R < 0, \quad R_1 > 0, \quad \Gamma, \Gamma_1, L_1 \text{ real}, \quad \text{regime I},$$

$$R > 0, \quad R_1 < 0, \quad \Gamma, \Gamma_1, L_1 \text{ imaginery}, \quad \text{regime II}. \tag{17}$$

This says that R and R_1 have opposite signs. In the solution obtained by Azaria and Giacomini [5], the final equivalent honeycomb Ising model is identical with ours except the replacement of R by $-R$. As we shall see in Eq. (21) below, the negations of R and/or R_1 do not affect the solution. Therefore, the two solutions are identical and this establishes that the two models in Figs. 1(a) and 1(b) are equivalent. In fact, by inverting spins surrounding the up-pointing (or down-pointing) triangular faces in every other row, the two models are transformed directly into each other.

Combining Eqs. (6), (9), and (16), and after some reduction, we obtain

$$F^4 = F_1^4 F_2^4 F_3^2 = \frac{4 \cosh^2 L (e^{4K_1} \sinh^2 L + \cosh^2 2K)}{\cosh^2 R_1}. \tag{18}$$

Now the field L_1 at the decorating sites is canceled [9] and we arrive at the final equivalence

$$Z_{\mathrm{KG}}(K,K_1,L) = F^N Z_{\mathrm{HC}}[R(L),R_1] \tag{19}$$

where $Z_{\mathrm{HC}}[R(L),R_1]$ is the partition function of the honeycomb Ising lattice. Here, N is the number of triangular faces (or the number of magnetic spins) of the kagome lattice, which is also the number of honeycomb lattice sites. Note that the L dependence is only in R.

The transformation (19) reduces to that of Fisher for the square lattice after setting $K_1=0(R_1=\infty)$. But our model differs from the Fisher model in a crucial aspect: The Fisher model results in a square lattice whose sites are the decorating sites of the original lattice, whereas in the present model all sites of the original kagome lattice disappear at the end. Thus the ordering of the honeycomb lattice bears no direct relationship to that of the kagome lattice. In addition, while there are no frustrated plaquettes in the Fisher model, in the $K_1>0$ model all triangular faces are frustrated.

Introduce the *per magnetic spin* free energy

$$f_{\mathrm{KG}}(K,K_1,L) = \lim_{N\to\infty} N^{-1} \ln Z_{\mathrm{KG}}(K,K_1,L)$$

and the per site honeycomb lattice free energy

$$f_{\mathrm{HC}}(R,R_1) = \lim_{N\to\infty} N^{-1} \ln Z_{\mathrm{HC}}(R,R_1). \tag{20}$$

Taking the $N\to\infty$ limit of Eq. (19) and making use of the explicit expression of f_{HC} given in [8,10], we obtain for the kagome Ising model,

$$f_{\mathrm{KG}}(K,K_1,L) = \ln F + f_{\mathrm{HC}}(R,R_1) = \ln F + \frac{3}{4}\ln 2 + \frac{1}{16\pi^2}\int_0^{2\pi} d\theta\, d\phi \ln \Xi(\theta,\phi) \tag{21}$$

where

$$\Xi(\theta,\phi) = \cosh 2R_1 \cosh^2 2R + 1 - \sinh^2 2R \cos(\theta+\phi) - \sinh 2R_1 \sinh 2R(\cos\theta + \cos\phi). \tag{22}$$

Note that the negation of either R or R_1 corresponds to changing $\theta\to\pi-\theta, \phi\to\pi-\phi$ in Eq. (22) which does not change the free energy f_{KG}.

As a check, we recover the Fisher solution [1] upon setting $K_1=0$ or $R_1\to\infty$:

$$f_{\mathrm{KG}}(K,0,L) = \frac{3}{2}\ln 2 + \frac{1}{4}\ln[\cosh^2 L(\sinh^2 L + \cosh^2 2K)] + \frac{1}{16\pi^2}\int_0^{2\pi} d\theta\, d\phi \ln[\cosh^2 2R - \sinh 2R(\cos\theta + \cos\phi)] \tag{23}$$

with $e^{-4R}=(\sinh^2 L+\cosh^2 2K)/\cosh^2 L$.

The internal energy and magnetization per magnetic spin are, respectively,

$$U(K,K_1,L) = -\frac{\partial}{\partial\beta} f_{\mathrm{KG}}(K,K_1,L), \tag{24}$$

$$M(K,K_1,L) = \frac{\partial}{\partial L} f_{\mathrm{KG}}(K,K_1,L). \tag{25}$$

The specific heat and susceptibility are further computed as

$$C_H(K,K_1,L) = \frac{\partial}{\partial T} U(K,K_1,L), \tag{26}$$

$$\chi(K,K_1,L) = \frac{\partial}{\partial H} M(K,K_1,L). \tag{27}$$

III. THE PHASE DIAGRAM

The integral in the free energy f_{KG} is precisely of the form of that of the free-fermion model discussed by Fan and Wu [6] for which the critical condition is (for $RR_1<0$)

$$\Xi(\pi,\pi) = 0. \tag{28}$$

Alternately, the critical point for an anisotropic honeycomb Ising lattice has been given in [10] as $C_1C_2C_3+1=S_1S_2+S_2S_3+S_3S_1$ where $C_i=\cosh 2R_i$, $S_i=\sinh|2R_i|$, $i=1, 2, 3$. It is also given by the expression $\omega_1=\omega_2+\omega_3+\omega_4$ [6] where the ω's are given in the next section. Using any of these expressions, we obtain the critical condition

$$\sinh[2R(L)] = -\coth R_1. \tag{29}$$

Explicitly, Eq. (29) reads

$$\cosh^2 L = \frac{1}{2}[\sqrt{1+\tanh^2 R_1} - 1] \times (e^{-4K_1}\cosh^2 2K - 1),$$

$$T = T_c(H), \tag{30}$$

which can be realized only in regime I and $K_1 \leqslant K$, or $\gamma \leqslant 1$ (see below). Note that for $K_1=0$ Eq. (30) reduces to the Fisher expression

$$\cosh L = \sqrt{(\sqrt{2}-1)/2}\, \sinh 2K. \tag{31}$$

It can be verified that we have

$$|\sinh 2R(L)| < |\coth R_1|, \quad T > T_c(H). \tag{32}$$

Introduce the parameters

$$\alpha = L/2K = H/2J > 0,$$

$$\gamma = J_1/J = K_1/K, \tag{33}$$

such that $\gamma>0$ indicates J_1 is ferromagnetic, and consider the phase diagram (30) in the $\{\alpha, 1/K\}$ plane, where $1/K$ is the temperature. The phase diagram is plotted in Fig. 3 for different fixed values of γ.

At low temperatures the phase boundary behaves as

$$\alpha = 1 - \gamma - \frac{1}{4K}\ln 2(\sqrt{2}+1) \tag{34}$$

with an initial slope independent of γ. Solving Eq. (30) for γ at $H=0$, we obtain

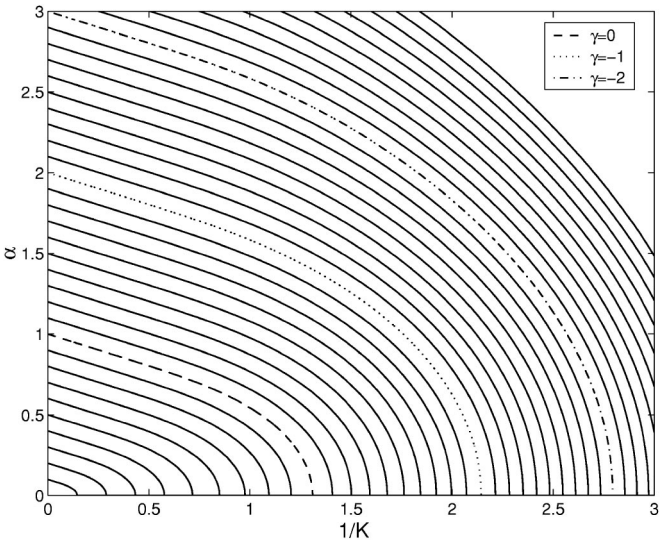

FIG. 3. Phase boundary in the $\alpha-1/K$ plane for fixed values of γ. $1/K$ is the temperature in units of J/k.

$$\gamma = \frac{1}{2K_c}[2\ln(\sinh 2K_c) - \ln(2\cosh 2K_c)]. \tag{35}$$

We see that $T_c(0)$ decreases with increasing γ, reaching $T_c(0)=0$ at $\gamma=1$. It follows that there is no transition when

$$\gamma \geqslant 1, \text{ or } K_1 \geqslant K \tag{36}$$

as aforementioned. This can be understood physically since, in the limit of $\gamma\to\infty$, the nonmagnetic spins can assume values ±1 randomly and there is no ordered state.

For small H Eq. (30) is expanded as

$$T_c(H) = T_c(0) - CH^2, \tag{37}$$

where C is a constant given by

$$C^{-1} = kJ\left[\frac{32(16-24t^4+t^8)}{t^9(4+4t^2-t^4)} + \frac{16(-4\gamma+4t+t^5)}{16-t^8}\right]$$

with $t=\tanh 2J/kT_c(0)$.

To determine the nature of regimes in the phase diagram, we consider the ground state. At zero temperature the kagome lattice can assume two ordered states.

(i) All magnetic spins are aligned in the same direction with the total energy

$$U_1 = -N(2\alpha+\gamma)J \tag{38}$$

independent of the spin directions of the nonmagnetic spins. Since the $N/2$ nonmagnetic spins can point in any direction, the entropy of this ground state is $\frac{1}{2}Nk\ln 2$.

(ii) The magnetic spins connected by interactions $-J$ assume the value $+1$ (or -1) and those connected by interactions $+J$ assume the value -1 (or $+1$), while all nonmagnetic spins are fixed at $+1$ (or -1). This forms a superexchange antiferromagnetic state with the energy

$$U_2 = -N(2-\gamma)J, \tag{39}$$

and the ground state is twofold degenerate with zero entropy in the thermodynamic limit.

Comparing U_1 with U_2, for $\alpha>1-\gamma$ which is the regime to the "exterior" of the critical curve (30), we have $U_1<U_2$, indicating the system is paramagnetic. For $\alpha<1-\gamma$, which is the regime enclosed by the critical curve, we have $U_1>U_2$, and the system assumes a superexchange antiferromagnetic ordering.

IV. THERMODYNAMIC PROPERTIES

In this and subsequent sections we carry out a detailed analysis of the thermodynamics of the partition function, which was not done in [5].

To analyze the thermodynamic and magnetic properties given by Eqs. (24)–(27), we make use of the results of [6]. Writing Eq. (22) in the form of Eq. (16) of [6], we have

$$\Xi(\theta,\phi) = 2a + 2b\cos\theta + 2c\cos\phi + 2d\cos(\theta+\phi), \tag{40}$$

with

$$a = \cosh 2R_1\cosh^2 2R + 1 = \frac{1}{2}(\omega_1^2+\omega_2^2+\omega_3^2+\omega_4^2),$$

$$b = -\sinh 2R_1\sinh 2R = \omega_1\omega_3 - \omega_2\omega_4,$$

$$c = -\sinh 2R_1\sinh 2R = \omega_1\omega_4 - \omega_{12}\omega_3,$$

$$d = -\sinh^2 2R = \omega_3\omega_4 - \omega_1\omega_2, \tag{41}$$

or

$$\omega_1 = \cosh(2R - R_1),$$

$$\omega_2 = \cosh(2R + R_1),$$

$$\omega_3 = \omega_4 = \cosh R_1. \tag{42}$$

Using Eq. (42) we compute the parameters $\{x,y,z\}$ introduced in [6] as

$$x = \omega_1\omega_4 - \omega_2\omega_3 = -\sinh 2R\sinh 2R_1,$$

$$y = \frac{1}{2}(\omega_1^2 - \omega_2^2 - \omega_3^2 + \omega_4^2) = -\frac{1}{2}\sinh 4R\sinh 2R_1,$$

$$z = \omega_1\omega_4 + \omega_2\omega_3 = 2\cosh 2R\cosh^2 R_1. \tag{43}$$

Here we have reversed the sign of x from [6] to make $x>0$. This is permitted since only x^2 appears in the ensuing discussions. The critical condition (29) is equivalent to $y=z$ and we have the regimes

$$y > z > x > 0, \quad T < T_c(H),$$

$$z > y > x > 0, \quad T > T_c(H). \tag{44}$$

It was established in [6] that derivatives of the free energy are best computed by first carrying out onefold integration. Adopting the notations in [6], we obtain after differentiating (21) the expression

$$[f_{\mathrm{KG}}(K,K_1,L)]' = C_0 + C_1 I_1 + C_2 I_2 + C_3 I_3, \tag{45}$$

where the prime denotes the derivative with respect to some variable such as T and H,

$$C_0 = \begin{cases} \dfrac{F'}{F} + \dfrac{b'}{4b}, |R_1| > |R| (b^2 > d^2), \\ \dfrac{F'}{F} + \dfrac{d'}{4d}, |R_1| < |R| (d^2 > b^2), \end{cases}$$

$$C_1 = a' - \frac{a}{2}\left(\frac{b'}{b} + \frac{d'}{d}\right) - \frac{b^2 - d^2}{4d}\left(\frac{b'}{b} - \frac{d'}{d}\right),$$

$$C_2 = \frac{b}{2}\left(\frac{b'}{b} - \frac{d'}{d}\right),$$

$$C_3 = -\frac{1}{2}\left(\frac{b'}{b} - \frac{d'}{d}\right)\frac{b^2 - d^2}{2d}\left(\frac{2ad}{b^2 + d^2} - 1\right), \tag{46}$$

and

$$I_1 = \frac{1}{8\pi}\int_0^{2\pi} d\phi [Q(\phi)]^{-1/2},$$

$$I_2 = \frac{1}{8\pi}\int_0^{2\pi} d\phi \cos\phi [Q(\phi)]^{-1/2},$$

$$I_3 = \frac{1}{8\pi}\int_0^{2\pi} d\phi (1 + \omega\cos\phi)^{-1} [Q(\phi)]^{-1/2} \tag{47}$$

with

$$\omega = -2bd/(b^2 + d^2) > 0,$$

$$Q(\phi) = x^2(\cos\phi - yz/x^2)^2 + (x^2 - y^2)(z^2 - x^2)/x^2. \tag{48}$$

Carrying out the integrations in Eq. (47), we obtain explicitly for $T \geqslant T_c(H) (z > y > x > 0)$ the result [11]

$$I_1 = \frac{1}{2\pi(z^2 - x^2)^{1/2}} K(k),$$

$$I_2 = \frac{1}{2\pi yz(z^2 - x^2)^{1/2}} [z^2 K(k) + (y^2 - z^2)\Pi(r,k)],$$

$$I_3 = \frac{1}{2\pi(y + \omega z)(z^2 - x^2)^{1/2}}\left(yK(k) + \frac{\omega(z^2 - y^2)}{z + \omega y}\Pi(s,k)\right), \tag{49}$$

where

$$k^2 = (y^2 - x^2)/(z^2 - x^2),$$

$$r = y^2/z^2,$$

$$s = (\omega z + y)^2/(z + \omega y)^2 \tag{50}$$

and K and Π are elliptical integrals of the first and third kinds, respectively,

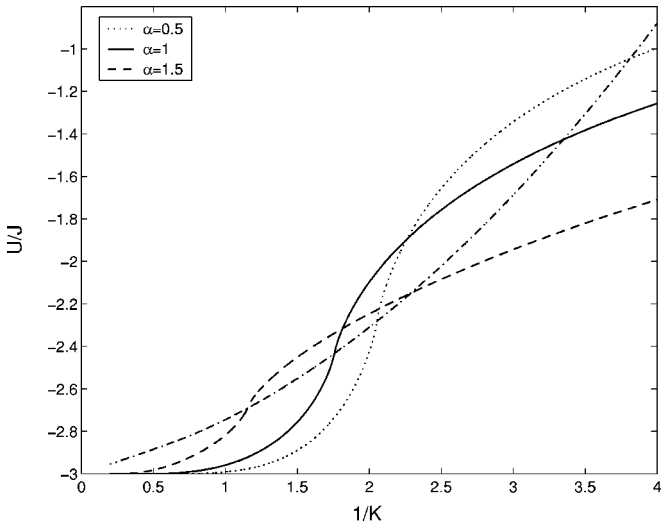

FIG. 4. Energy U versus temperature T (in units of J/k) at fixed magnetic field H for $\gamma = -1$. The dot-dashed line indicates the critical energy U_c.

$$K(k) = \int_0^{\pi/2} \frac{d\alpha}{\sqrt{1 - k^2\sin^2\alpha}},$$

$$\Pi(r,k) = \int_0^{\pi/2} \frac{d\alpha}{(1 - r\sin^2\alpha)\sqrt{1 - k^2\sin^2\alpha}}. \tag{51}$$

For $T \leqslant T_c(H) (y > z > x > 0)$ we obtain the same result with y and z interchanged.

The apparent nonanalyticity of C_0 at $|R_1| = |R|$ as indicated in Eq. (46) is spurious. It can be shown that the combination of $C_0 + C_3 I_3$ is always analytic.

At the transition temperature $y = z$ (or $k = 1$, $r = 1$) both K and Π diverge as $\ln|T - T_c(H)|$. Applying Eq. (45) to the internal energy (24) where the derivatives are with respect to T, we obtain

$$U(H) = U_c(H) + \mathrm{const}|T - T_c(H)|\ln|T - T_c(H)|,$$

$$T \to T_c(H). \tag{52}$$

A further derivative of $U(H)$ as given by Eq. (26) gives the specific heat C_H. Thus, the energy is continuous at $T_c(H)$ while the specific heat diverges logarithmically. These findings, which are the same as those found in the Fisher model, indicate the occurrence of a second-order transition along the phase boundary in Fig. 3. We plot $U(H)$ and C_H respectively in Figs. 4 and 5. For completeness, we derive the explicit expression for $U_c(H)$ in the next section.

In the case of zero magnetic field $H = \alpha = 0$ and $\gamma = -1$, the internal energy assumes a simple expression given by

$$U(0)/J = -1 + (1 + \tanh 2K)\left(1 - \frac{1}{2}\tanh R - [1 + 2(\cosh^3 2R - 3\cosh 2R - 2)I_1]\coth 2R\right) \tag{53}$$

with $e^{-2R} = e^{2R_1} = (e^{4K} + 1)/2$.

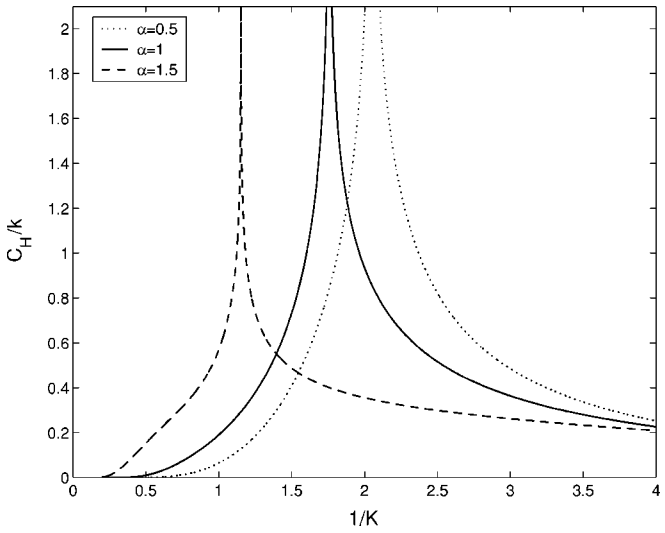

FIG. 5. Specific heat C_H as a function of temperature T (in units of J/k) at fixed magnetic field H for $\gamma=-1$.

V. DERIVATION OF $U_c(H)$

Define an auxiliary variable

$$\varphi_\alpha(k)=\sin^{-1}\sqrt{\frac{1-\alpha}{1-k^2}}>0$$

which gives, for k^2, r, s given in Eq. (50),

$$\varphi_r(k)=\sin^{-1}\sqrt{1-\frac{x^2}{z^2}},$$

$$\varphi_s(k)=\sin^{-1}\sqrt{\frac{(1-\omega^2)(z^2-x^2)}{(z+\omega y)^2}},$$

$$\varphi_s(1)=\sin^{-1}\sqrt{\frac{1-\omega}{1+\omega}\left(1-\frac{x^2}{z^2}\right)},\quad T=T_c(H), \tag{54}$$

where the last line holds at the critical temperature $k=1$ or $y=z$.

For $k^2<r<1$ we have [12]

$$\Pi(r,k)=K(k)+\frac{\pi}{2}\sqrt{\frac{r}{(1-r)(r-k^2)}}[1-\Lambda_0(\varphi_r,k)]$$

where Λ_0 is Heuman's Lambda function

$$\Lambda_0(\varphi,k)=\frac{2}{\pi}[K(k)E(\varphi,k')-[K(k)-E(k)]F(\varphi,k')] \tag{55}$$

with $k'=\sqrt{1-k^2}$ and

$$E(\varphi,k)=\int_0^\varphi (1-k^2\sin^2\theta)^{1/2}d\theta,$$

$$F(\varphi,k)=\int_0^\varphi (1-k^2\sin^2\theta)^{-1/2}d\theta. \tag{56}$$

Particularly,

$$\Lambda_0(\varphi,1)=\frac{2}{\pi}\varphi. \tag{57}$$

At the critical point $k\to 1$ or $y\to z$, we have

$$(z^2-y^2)\Pi(r,k)=(z^2-y^2)K(k)+\frac{\pi z^2(z^2-x^2)^{1/2}}{2x}\left(1-\frac{2}{\pi}\varphi_r\right), \tag{58}$$

$$(z^2-y^2)\Pi(s,k)=(z^2-y^2)K(k)+\frac{\pi(1+\omega)z^2(z^2-x^2)^{1/2}}{2\sqrt{(1-\omega)[(1-\omega)x^2-2\omega z^2]}}\left(1-\frac{2}{\pi}\varphi_s\right), \tag{59}$$

and

$$I_2=I_1-\frac{1}{4x}\left(1-\frac{2}{\pi}\varphi_r\right),$$

$$I_3=\frac{1}{1+\omega}\left[I_1+\frac{\omega}{4\sqrt{(1-\omega)[(1-\omega)x^2+2\omega z^2]}}\left(1-\frac{2}{\pi}\varphi_s\right)\right]. \tag{60}$$

Let

$$q=\sinh^2 R_1 \gtrless \frac{1}{2},\quad |R_1|\gtrless |R|.$$

Then, at the critical temperature $T_c(H)$

$$\omega=\frac{4q}{1+4q^2},\quad x=2(1+q),$$

$$y^2=z^2=4(1+q)^2(1+2q)/q,$$

$$\varphi_r=\sin^{-1}\sqrt{\frac{1+q}{1+2q}}$$

$$\varphi_s=\sin^{-1}\left[\frac{|2q-1|}{2q+1}\sqrt{\frac{1+q}{1+2q}}\right],$$

$$I_2=I_1-\frac{1}{8(1+q)}\left(1-\frac{2}{\pi}\varphi_r\right),$$

$$I_3=\frac{1+4q^2}{(1+2q)^2}\left[I_1+\frac{q}{2(1+q)|1-2q|(2q+3)}\left(1-\frac{2}{\pi}\varphi_s\right)\right], \tag{61}$$

and

$$C_1=-\frac{(q+1)(4q^2+8q-3)}{2q}\times\left(\coth 2R_1\frac{\partial R_1}{\partial K}-\coth 2R\frac{\partial R}{\partial K}\right),$$

$$C_2=-2(1+q)\left(\coth 2R_1\frac{\partial R_1}{\partial K}-\coth 2R\frac{\partial R}{\partial K}\right),$$

$$C_3 = \frac{(q+1)(2q-1)(2q+3)(2q+1)^2}{2q(4q^2+1)} \times \left(\coth 2R_1 \frac{\partial R_1}{\partial K} - \coth 2R \frac{\partial R}{\partial K} \right), \tag{62}$$

where

$$\frac{\partial R_1}{\partial K} = \frac{2(e^{-4\gamma K_c}\sinh 4K_c - \gamma)}{e^{-4\gamma K_c}\cosh 4K_c - 1} + \frac{2\gamma}{e^{-4\gamma K_c} - 1},$$

$$\frac{\partial R}{\partial K} = -\frac{e^{-4\gamma K_c}(\sinh 4K_c - 2\gamma \cosh^2 2K_c) + \alpha \sinh 4\alpha K_c}{2(\sinh^2 2\alpha K_c + e^{-4\gamma K_c}\cosh^2 2K_c)} + \alpha \tanh 2\alpha K_c \tag{63}$$

where $K_c = J/kT_c(H)$. Combining these results, we obtain after some algebra the following expression for the energy at the critical temperature:

$$U_c(H)/J = -\gamma - 2\alpha \tanh 2\alpha K_c - \frac{1}{2\sinh 2R_1}\frac{\partial R_1}{\partial K} + \frac{1}{2}(2 - \coth 2R)\frac{\partial R}{\partial K} + \frac{1}{2\pi}(\varphi_r \pm \varphi_s)\left(\coth 2R_1 \frac{\partial R_1}{\partial K} - \coth 2R \frac{\partial R}{\partial K} \right),$$

$$q \gtrless \frac{1}{2}. \tag{64}$$

In the limit of $\gamma \to 0$ for which $R_1 \to \infty$, $\varphi_r = \varphi_s = \pi/4$, we obtain

$$U_c(H)/J_{\gamma=0} = -(2-\sqrt{2})\alpha \tanh 2\alpha K_c - \frac{1}{2-\sqrt{2}} \frac{\sinh 4K_c + \alpha \sinh 4\alpha K_c}{\sinh^2 2\alpha K_c + \cosh^2 2K_c} \tag{65}$$

which is the Fisher result [1]. Particularly, for $H=0$, Eq. (65) gives the value $-2\sqrt{1+\sqrt{2}}$.

VI. MAGNETIC PROPERTIES

For magnetic properties we take the derivative in Eq. (45) with respect to H and obtain

$$M(H) = M_c(H) + \text{const} \times |T - T_c(H)| \ln |T - T_c(H)|, \quad T \to T_c(H), \tag{66}$$

where $M_c(H)$ is the magnetization at the critical temperature $T_c(H)$ given by

$$M_c(H) = \frac{1}{2}\left[1 - \frac{1}{\pi}(\varphi_r \pm \varphi_s) \right](1 + e^{4R}) \tanh 2\alpha K_c, \quad q \gtrless \frac{1}{2}. \tag{67}$$

The magnetization M is plotted in Figs. 6 and 7 versus T and H, respectively, for $\gamma = -1$. To analyze $M(H)$

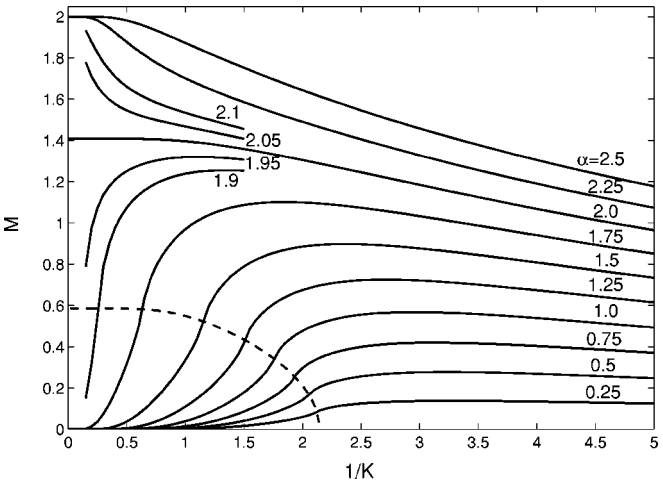

FIG. 6. Magnetization M versus temperature T (in unit of J/k) at fixed magnetic field H for $\gamma = -1$. The broken line indicates $M_c(H)$.

$\equiv M(\gamma, \alpha, 1/K)$ at low temperatures, we note that

$$M(\gamma, \alpha, 0) = \begin{cases} 0, \alpha < 1 - \gamma, \\ 2, \alpha > 1 - \gamma. \end{cases} \tag{68}$$

The value of $M(\gamma, \alpha, 0)$ at $\alpha = 1 - \gamma$ depends on how the zero temperature $T=0$ is approached. To see what happens we write

$$\alpha(K, \xi) \equiv 1 - \gamma - \frac{\xi}{4K} \ln 2(\sqrt{2}+1) \tag{69}$$

where ξ is a parameter controlling the approach to $T=0$. Particularly, the critical curve (34) is indicated by $\xi = 1$. Along Eq. (69) and $K \to \infty$, one has $R_1 \simeq 2K \to \infty$, $\tanh L \to 1$, and

$$e^{-4R} = 1 + [2(\sqrt{2}+1)]^{\xi}, \quad K \to \infty.$$

After some algebraic manipulation, we find

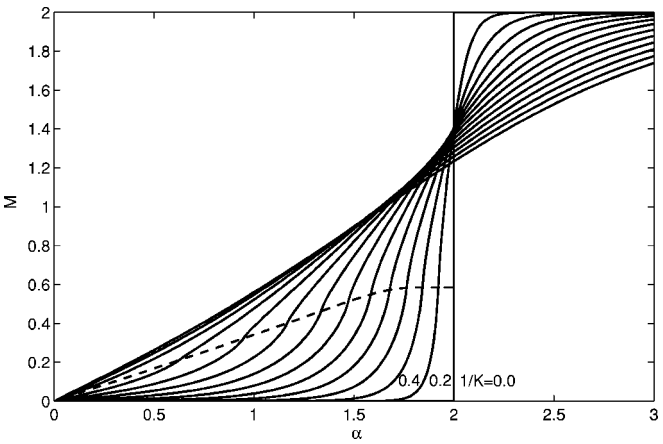

FIG. 7. Magnetization M versus magnetic field $\alpha = H/2J$ at fixed temperature T for $\gamma = -1$. The broken line indicates $M_c(H)$.

$$m(\xi) \equiv \lim_{K\to\infty} M(\gamma,\alpha(K,\xi),1/K) = (e^{4R}+1)\left[\frac{1}{2}+\frac{\epsilon}{\pi}(1 - k)K(k)\right] \tag{70}$$

with $k=\sinh^{2\epsilon}2R$. Here $\epsilon=1$ for $\xi\leqslant 1$ while $\epsilon=-1$ for $\xi>1$. We have

$$\begin{aligned} m(\xi) &= 0 \quad (\xi=\infty) \\ &= 2-\sqrt{2} \quad (\xi=1) \\ &= \frac{3}{4}+\frac{21}{16\pi}K\left(\frac{1}{8}\right) \\ &\simeq 1.408\,836 \quad (\xi=0) \\ &= 2 \quad (\xi=-\infty). \end{aligned} \tag{71}$$

The susceptibility $\chi(\gamma,\alpha,K^{-1})$, which is the further derivative of (66) with respect to H, diverges logarithmically at $T_c(H)$ for $H\neq 0$. The susceptibility χ is plotted in Fig. 8 versus temperature T for $\gamma=-1$ and $\alpha=0,1/2$. The zero-field susceptibility $\chi(\gamma,0,K^{-1})$ is continuous. For example one has for $\gamma=-1$,

$$\begin{aligned} \chi(-1,0,K^{-1}) = 2K - \frac{K}{2}(1-e^{4R})\Big\{ & 2-\frac{3}{2}\coth 2R \\ & + \coth 2R[2\cosh 2R(3-\sinh^2 2R)+6]I_1 \\ & + \sinh 4R\, I_2\Big\} \end{aligned} \tag{72}$$

where $e^{-2R}=(e^{4K}+1)/2$. The expression (72) bears no direct relation to the critical energy (53) as found to exist in the case of $\gamma=0$ [1]. By direct differentiation of Eq. (67) and making use of Eq. (37), we obtain the critical susceptibility

$$\chi(\gamma,0,K_c^{-1}) = \frac{1}{2}K_c\left[1-\frac{1}{\pi}(\varphi_r \pm \varphi_s)\right] \times (1+e^{4\gamma K_c}\cosh^{-2}2K_c), \quad q \gtrless \frac{1}{2}. \tag{73}$$

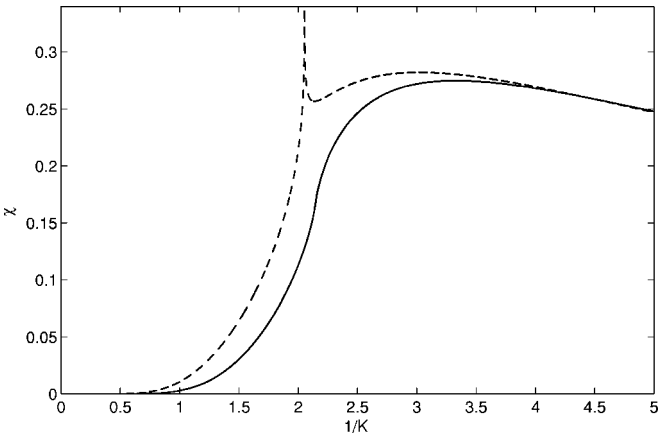

FIG. 8. Susceptibility χ in units of $1/J$ as a function of temperature T (in units of J/k) for $\gamma=-1$. Solid line $H=0$. Broken line $H=J(\alpha=1/2)$.

ACKNOWLEDGMENTS

We thank R. Shrock for his interest and a critical reading of the manuscript. Work has been supported in part by NSF Grants No. PHY-0098801 (W.T.L.) and No. DMR-9980440 (F.Y.W.).

[1] M. E. Fisher, Proc. R. Soc. London, Ser. A **254**, 66 (1960); **256**, 502 (1960).
[2] H. Giacomini, J. Phys. A **21**, L31 (1988).
[3] K. Y. Lin, J. Phys. A **22**, 3435 (1989).
[4] K. Obredors, A. Labarta, A. Isaigue, J. Tejeda, J. Rodrigues, and M. Pernet, Solid State Commun. **65**, 189 (1988).
[5] P. Azaria and H. Giacomini, J. Phys. A **21**, L935 (1988).
[6] C. Fan and F. Y. Wu, Phys. Rev. B **2**, 723 (1970).
[7] I. Syozi, Prog. Theor. Phys. **6**, 306 (1951).
[8] I. Syozi, in *Phase Transitions and Critical Phenomena*, edited by C. Domb and M. S. Green (Academic Press, New York, 1972), Vol. 1.
[9] The cancellation of the resulting fields also holds if the external magnetic field assumes different values along different rows of the black circles in Figs. 1(a) and 1(b), resulting in honeycomb Ising lattice with different local interactions.
[10] R. M. F. Houtappel, Physica (Amsterdam) **16**, 425 (1950).
[11] The expressions of I_1, I_2, I_3 given just above Eq. (41) in [6] contain the following typos. The arguments g of the elliptical integrals should read q. In the expression of I_1 replace $(z^2-x^2)\to(z^2-x^2)^{1/2}$, in the expression of I_2 multiply the whole expression by $1/z$, and in the expression of I_3 replace the first g by y.
[12] *Handbook of Mathematical Functions with Formulas, Graphs, and Mathematical Tables*, edited by M. Abramowitz and I. A. Stegun, Nat. Bur. Stand., Appl. Math. Ser. No. 55, (U.S. GPO, Washington, DC, 1970), Eqs. (17.7.14) and (17.4.40).